Journal of Fluorine Chemistry 131 (2010) 417–425

Contents lists available at ScienceDirect

Journal of Fluorine Chemistry

journal homepage: www.elsevier.com/locate/fluor

Preparation and characterization of fluorinated acrylate copolymer latexes by miniemulsion polymerization under microwave irradiation

Shengdong Xiong [a], Xiaoli Guo [a], Ling Li [a], Shuilin Wu [a,b], Paul K. Chu [b,*], Zushun Xu [a,b,**]

[a] Ministry-of-Education Key Laboratory for the Green Preparation and Application of Functional Materials, Hubei University, Wuhan 430062, China
[b] Department of Physics & Materials Science, City University of Hong Kong, Tat Chee Avenue, Kowloon, Hong Kong, China

ARTICLE INFO

Article history:
Received 23 October 2009
Received in revised form 15 December 2009
Accepted 16 December 2009
Available online 23 December 2009

Keywords:
Miniemulsion polymerization
Fluorinated acrylate
Microwave irradiation
Microstructure
Kinetics

ABSTRACT

Fluoroacrylate copolymer miniemulsion was prepared by miniemulsion polymerization under microwave irradiation. The composition of the copolymer was determined by FTIR, DSC, ^{1}H NMR and ^{19}F NMR. The morphology, size, and size distribution of the latex particles as well as changes in the size during polymerization were characterized by TEM and photon correlation spectroscopy (PCS). The effects of kinetic parameters on the polymerization were evaluated. The particle size of latex underwent almost no change during microwave irradiation polymerization. The diameters of latex particles prepared by microwave irradiation were smaller and more monodispersed than those prepared by conventional heating and the latex had good centrifugal stability. Polymerization under microwave irradiation had a higher reaction rate and higher conversion than traditional heating. By using 10 wt% fluoromonomer, the surface energy of the latex film could be reduced from 27.24 mJ/m^2 (latex film of fluorine-free) to 17.59 mJ/m^2 and the decomposition temperature increased by 25 °C.

1. Introduction

Fluorinated polymers are known to have many useful and desirable features such as unique surface/optical properties, high thermal stability, superb chemical resistance, excellent mechanical properties at extreme temperatures owing to the low polarizability and the strong electronegativity of fluorine atom [1,2]. Acrylic polymers with fluorine-containing groups or perfluoroalkyl groups, in particular, can provide the material with low surface energies and the acrylic groups ensure that the polymers can adhere well to various substrates [3,4]. Therefore, fluorinated polyacrylate latexes have been used progressively in a wide range of applications such as biomaterials, microelectronics, antifogging, and antifouling applications [5–7], especially as surface coatings for textile, paper and leather, because their presence can introduce a number of unique physical and chemical surface properties [1,8]. Many fluorinated or perfluorinated (meth)acrylate monomers have been studied with regard to the synthesis of copolymers with conventional acrylate in aqueous emulsions by radical polymerization methods [1,5–10]. Most of them are the copolymers of fluorinated acrylate with long perfluoroalkyl groups (>7 fluorocarbons). However, poly (fluoroalkyl acrylates) with long perfluoroalkyl groups have been found to degrade to form perfluorooctanoic acid (PFOA), which can resist degradation and bioaccumulate in the human body [11,12]. But the properties of fluorinated polyacrylate latexes which contain long fluoroalkyl groups are better than those containing short-chain fluoroalkyl groups [13]. Hence, the perfluoroalkyl acrylate with short fluorinated side chain (<7 fluorocarbons) and have relatively more number of fluorine atoms becomes alternative fluorinated materials to avoid the adverse reaction associated with PFOA.

In a classical emulsion polymerization technique the monomer relies on transport from the droplets to the growing particles. However, because the solubility of fluorinated monomers in water is very low [7,14–17], therefore, FA-containing copolymer latexes are usually synthesized by the addition of a large quantity of an organic solvent to the continuous phase [7,14] or in supercritical carbon dioxide [18] or by use of some special emulsifier such as cationic surfactant [17], polymerizable emulsifier [19]. Miniemulsion polymerization is an *in situ* method to prepare fluorinated acrylate copolymers because of the unique features. In miniemulsion polymerization, both the particle nucleation and subsequent propagation reaction occur primarily in submicrometer monomer droplets of 50–500 nm. Polymerization in miniemulsion does not depend on the monomer transport through the water phase. The predominant initiation mechanism is droplet nucleation in which

* Corresponding author. Tel.: +852 34427724; fax: +852 27889549.
** Corresponding author at: Ministry-of-Education Key Laboratory for the Green Preparation and Application of Functional Materials, Hubei University, Wuhan 430062, China. Tel.: +86 27 61120608; fax: +86 27 88665610.
E-mail addresses: paul.chu@cityu.edu.hk (P.K. Chu), zushunxu@hubu.edu.cn (Z. Xu).

0022-1139/$ – see front matter © 2009 Elsevier B.V. All rights reserved.
doi:10.1016/j.jfluchem.2009.12.015

each small stabilized droplet in the minimeulsion can be regarded as a nanoreactor [15,20–22]. This enables polymerization of the miniemulsions, and the problem associated with polymerization of extremely hydrophobic fluoromonomers can be simplified to the successful preparation stable miniemulsions while solubility questions are avoided. Fluorinated monomers produced by miniemulsion polymerization have been reported [7,15,23,24].

Microwave radiation as a fast and efficient means to heat the reaction media has significant advantages over conventional thermal methods. Studies have shown that in comparison with reactions under conventional heating, reactions under microwave irradiation have the advantages of higher reaction rates and higher monomer conversion in a shorter period of time [25–27]. Recently, many researchers have focused on polymerization with microwave irradiation [28–30]. Hoogenboom and Schubert have reviewed the applications of microwave irradiation to polymer chemistry [31]. Concerning the mechanism of miniemulsion polymerization, the major interest in miniemulsion polymerization is droplet nucleation to avoid micellar nucleation because polymerization inside a droplet starts as soon as a radical enters. Therefore, miniemulsion polymerization seems to be particularly suitable for the combination utilizing a very fast microwave heating. In this way, microwave heating may provide ultra-fast processing assuming that the nucleation step does become rate-limiting.

So far, miniemulsion polymerization under microwave irradiation has not been investigated extensively. Holtze [32,33] and Zhu [34] have indeed conducted some research on the use of microwave irradiation in miniemulsion polymerization. Holtze [32,33] indicated that ultra-fast conversion and molecular weight could be obtained through temperature programming in microwave induced miniemulsion polymerization. In Zhu's work [34], well-defined and stable polystyrene latexes were obtained by nitroxide-mediated radical miniemulsion polymerization under microwave irradiation.

In this work, we first applied microwave irradiation to the miniemulsion copolymerization of fluoroacrylate. Dodecafluoroheptyl methacrylate (DFHMA) (<7 fluorocarbons and has 11 fluorine atoms) was adopted as a fluorine-containing monomer. The particle morphology and size change during miniemulsion polymerization were determined. The effects of operation parameters such as temperature, concentration of initiator and emulsifier on monomer conversion were investigated systematically. The surface properties and thermal stability of the latex films were also characterized by contact angle, atomic force microscopy (AFM) and thermo-gravimetric analyses.

2. Results and discussion

2.1. Composition and structure of the copolymer

Fig. 1 shows the FTIR spectrum of the MMA–BA copolymer (A) and DFHMA–MMA–BA (B). In these two spectra, the characteristic absorption by the C=C bond at 1640 cm^{-1} disappears, indicating that the monomers polymerize. The characteristic stretching peaks of C–H and C=O group are obviously shown at 2850–3000 and 1732 cm^{-1}, respectively, resulting from that BA, MMA and DFHMA all contain CH_2 and C=O groups. In comparison with the FTIR spectrum of MMA–BA copolymer (A), the FTIR absorption peaks at 1000–1260 cm^{-1} in the spectrum of DFHMA–MMA–BA copolymer (B) are wider and blunter because of the overlap between the stretching vibration absorption of the C–F bond at 1100–1260 cm^{-1} and the stretching vibration absorption of the C–O–C bond at 1250 cm^{-1}. In the fingerprint region, there are two medium bands at 660 and 710 cm^{-1} resulting from a combination of rocking and wagging vibration of CF_3 groups.

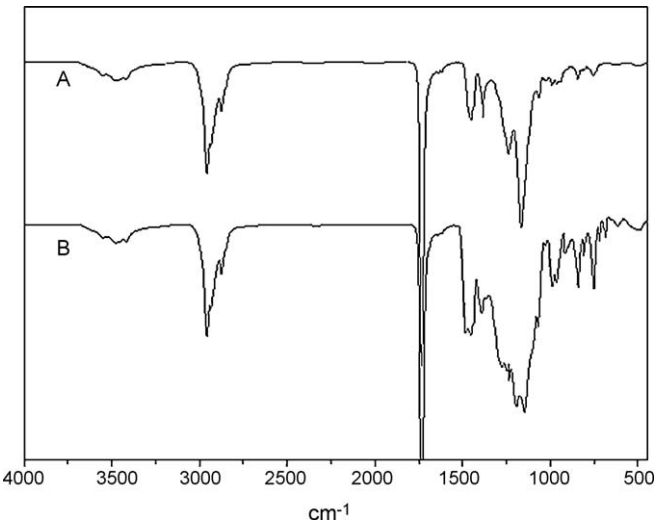

Fig. 1. FTIR spectra of (A) MMA–BA copolymer (MMA, 4.00 g; BA, 3.50 g) and (B) DFHMA–MMA–BA copolymer (DFHMA, 2.50 g; MMA, 4.00 g; BA, 3.50 g).

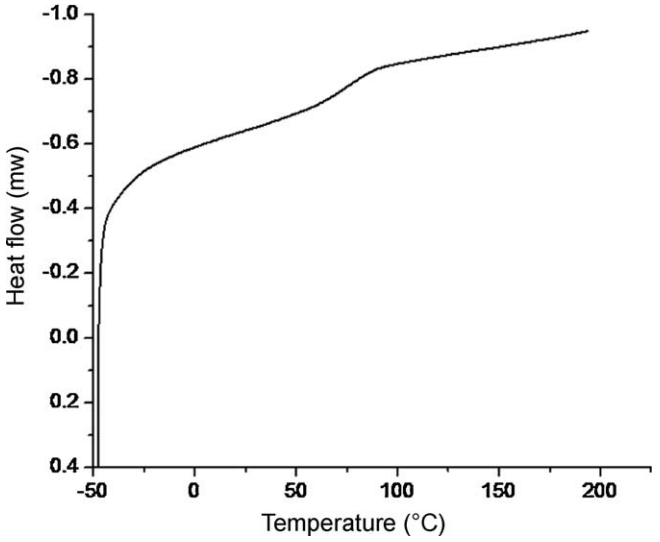

Fig. 2. DSC curve of DFHMA–MMA–BA copolymer (DFHMA, 2.50 g; MMA, 4.00 g; BA, 3.50 g).

Fig. 2 illuminates the DSC curve of the DFHMA–MMA–BA copolymer. As shown in Fig. 2, only one glass transition (76 °C) appeared on the curve, indicating that a random fluorinated acrylate copolymer was obtained.

To better characterize the structure of the copolymer, ^1H NMR and ^{19}F NMR are used to determine the fluorinated acrylate copolymer. The ^1H NMR spectrum of the fluorinated acrylate copolymer and peak assignments is presented in Fig. 3. The signals due to terminal methyl group protons are seen at approximately δ 0.75–1.15 ppm (t, 3H). The signal of methylene protons ($-CH_2-$) in the copolymer backbone is observed at approximately δ 1.5–2.2 ppm (m, 2H), and the peak at δ 3.63 ppm (m, 3H) is indicative of the $-OOCH_3$ group of MMA. The $-COOCH_2-$ peak at δ 4.15 ppm (t, 2H) due to the DFHMA and BA in the polymer chain is observed, and another peak at δ 4.09 ppm (s, H) is assigned to Rf–CHF–. The signal of methylene protons ($-(CH_2)_2-$) of BA is observed at approximately δ 1.15–1.5 ppm (m, 2H). No signals for the protons associated with double bond of unreacted DFHMA, BA and MMA can be detected in this ^1H NMR spectrum. The ^{19}F NMR spectrum of the copolymers depicted in Fig. 4 confirms the presence of three

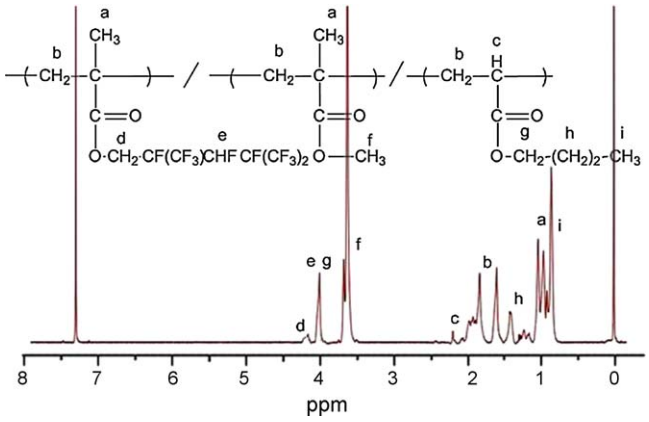

Fig. 3. ^{1}H NMR spectrum of DFHMA–MMA–BA copolymer (DFHMA, 2.50 g; MMA, 4.00 g; BA, 3.50 g).

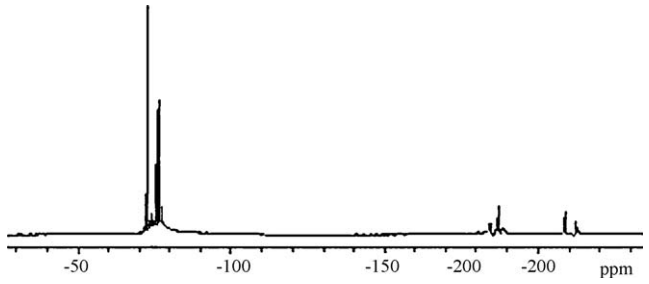

Fig. 4. ^{19}F NMR spectrum of DFHMA–MMA–BA copolymer (DFHMA, 2.50 g; MMA, 4.00 g; BA, 3.50 g).

different kinds of fluorine resonances originating from the DFHMA side chains. The chemical shifts are −72.5 to −78.5 ppm (t, 3F) of –CF_3 group, −184 to −188 ppm (d, F) of –CHF– group, and −208 to −212 ppm of –CH_2CF– group, respectively. These FTIR, ^{1}H NMR and ^{19}F NMR results confirm that the fluorinated acrylate copolymer have been successfully prepared.

2.2. Size and morphology of the latex particles

Table 1 shows the average particle size during the microwave irradiation miniemulsion polymerization process. The average particle size remains almost constant, and the final polymer particles are found in the manner of a one-to-one copy of the monomer droplets. In ideal miniemulsion polymerization, no monomer transport is involved and the latex particles have about the same size as the initial monomer droplets. As shown in Table 1, the size of final particles decreases from 98.5 nm to 72.3 nm when the amount of emulsifier increases from 1.5 wt% to 4.5 wt% (weight percentage of the emulsifier with respect to the monomer mixture). With a higher amount of emulsifier, the initial monomer droplets increases on the one hand and so the particle size of monomer droplets decreases, but on the other hand, more emulsifier will cover the surface of the droplets and therefore the resultant polymer particles can be in the manner of a one-to-one copy of the monomer droplets finally forming the small particles.

Table 1
Characteristics of latex particles size prepared by miniemulsion polymerization under microwave irradiation using different amounts of emulsifier (DFHMA, 2.50 g; MMA, 4.00 g; BA, 3.50 g; AIBN, 0.05 g, microwave irradiation at 80 °C, 400 W).

Samples	Emulsifer (wt%)	Diameters of particles size (nm)			
		0 min	40 min	80 min	120 min
1	1.5	102.6	96.8	99.8	98.5
2	2.5	95.5	86.3	86.5	86.9
3	3.5	94.0	76.4	76.9	76.9
4	4.5	77.9	72.6	73.6	72.3

Table 2
Effects of the amount of DFHMA on the particle size and centrifugal stability of the miniemulsion (the miniemulsion was prepared by microwave irradiation at 80 °C, 400 W).

Amount of DFHMA (wt%)	0	5	10	15	25
Diameters of particles size (nm)	70.8	73.7	80.1	84.3	86.9
Sedimentation ratio (wt%)	1.34	4.24	6.79	8.91	11.63

Further research was carried out on the effect of the amount of DFHMA (weight percentage of the DFHMA with respect to the monomer mixture) on the final particle size. The results are shown in Table 2. As shown in Table 2, with increasing the ratio of DFHMA, the particle size increased slightly. This may be due to the more fluorine segment, the greater the hydrophobic force around the particles, then the particles were more prone to secondary or higher levels of aggregation lead to the increase of particle size [13].

Fig. 5 shows typical TEM images of the latex particles obtained by (A) conventional heating miniemulsion polymerization (microwave irradiation at 80 °C, 400 W for 2 h) and (B) microwave irradiation miniemulsion polymerization (carried out at 80 °C for 8 h). As shown in Fig. 5, the latex particles obtained by the two methods have a spherical morphology. The D_n, D_w, and *PDI* values of the latex particles prepared by conventional heating miniemulsion polymerization (A) are 75.5 nm, 81.2 nm, and 1.0755, respectively corresponding to the hydrodynamic diameters and size distribution of latex particles estimated by PCS to be 112.3 nm and 1.1234. The hydrodynamic diameters are a little larger than those estimated by TEM. It is believed to arise from the presence of water in the PCS experiments inducing swelling of the particles. In addition, the D_n, D_w, and *PDI* values of the latex particles prepared by microwave irradiation miniemulsion polymerization (B) are 56.7 nm, 58.5 nm, and 1.0317, respectively, and the hydrodynamic diameters and size distribution of latex particles estimated by PCS are 86.9 nm and 1.0335.

According to the TEM images in Fig. 5, the latex particles prepared with microwave irradiation are much smaller than those prepared by conventional heating. Furthermore, the size distribution of the latex particles prepared by microwave irradiation is narrower than that of that prepared by conventional heating.

During microwave irradiation, absorption and transmission of energy are completely different from those in conventional heating. Energy transfer is produced not by conduction or convection, but by dielectric loss. The microwave energy is delivered to the interior of the heated materials and so the interior of the materials can be heated without conductive heating. In microwave irradiation miniemulsion polymerization, microwave irradiation plays a main role in enhancing the activity of the initiator AIBN by raising its decomposition and accelerating the polymerization process. The initiation efficiency of AIBN can be enhanced and the formation rate of the primary active species in the monomer droplets increases with accelerated decomposition rates of AIBN. Hence, large amounts of active species are formed under microwave irradiation in monomer droplets in a short time. The chance of monomer transport and aggregation of primary active particles decreases and so the size of the latex particles is smaller than that prepared by conventional heating. The size distribution of the latex particles is also reduced. Furthermore, large amounts of active species form in the monomer droplets under microwave irradiation in a short time. As a result, droplet

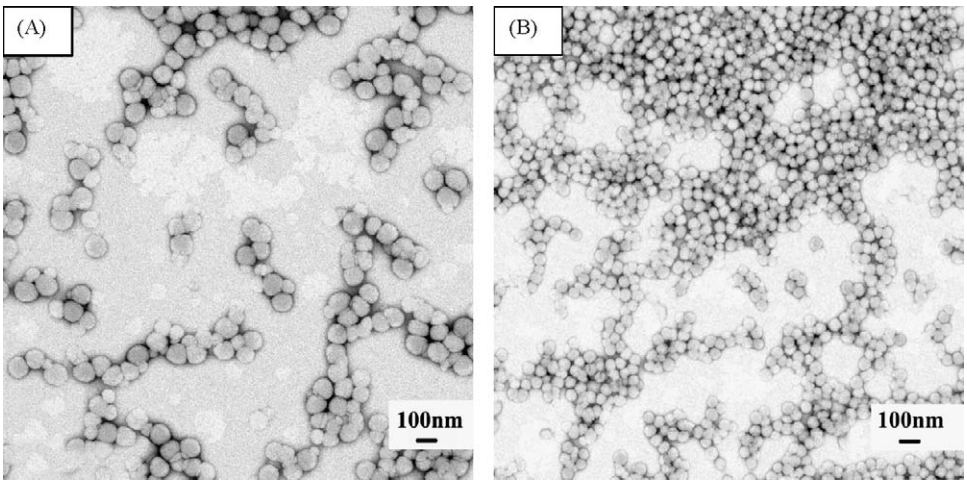

Fig. 5. TEM images of copolymer latexes prepared by miniemulsion polymerization: (A) conventional heating at 80 °C for 8 h and (B) microwave irradiation at 80 °C, 400 W for 2 h (DFHMA, 2.50 g; MMA, 4.00 g; BA, 3.50 g; HD, 0.40 g; OP-10, 0.17 g; SDS, 0.08 g; AIBN, 0.05 g; H_2O, 40.00 g).

nucleation is the predominant initiation mechanism in the microwave irradiation miniemulsion polymerization system, and each miniemulsion droplet can be perceived as a separate nanoreactor that does not interact with others. According to the general mechanism of miniemulsion polymerization, polymerization is more efficient under microwave irradiation.

2.3. Effects of kinetic parameters on polymerization

Fig. 6 illustrates the effects of the temperature on the monomer conversion in miniemulsion polymerization. In miniemulsion polymerization, droplet nucleation is dominant. Almost all the monomer droplets are initiated at the same time and monomer diffusion and transport are limited. Therefore, the influence of temperature on miniemulsion polymerization is small. The final monomer conversion and polymerization rate increase with reaction temperature. The reaction rate (R_p) is calculated by formula $R_p = (dc/dt)[M_0]$, where R_p is the reaction rate, dc/dt is differential time–conversion curve, and $[M_0]$ is the initial concentration of the monomer. The relationship of ln R_p versus $1/T$ is illustrated in Fig. 7. According to the Arrhenius equation, the apparent activation energy of miniemulsion polymerization under microwave irradiation is 45.7 kJ/mol whereas the value obtained by conventional heating is 76.3 kJ/mol. Fig. 6 also indicates that at 80 °C, the monomer conversion under microwave irradiation can reach 80% in 10 min, whereas it is only 35% by conventional heating. The final conversion efficiency by microwave irradiation is 97% which is higher than the final conversion rate of 65% by conventional heating. In other words, miniemulsion copolymerization under microwave irradiation yields a higher reaction rate and more effective conversion than traditional heating. This is due to the large amounts of active species formed by microwave irradiation in the monomer droplets in a short time thereby enhancomg the rate of the polymerization and increasing the conversion.

Fig. 8 illustrates the effect of the amount of emulsifier (weight percentage of the emulsifier with respect to the monomer mixture) on the miniemulsion copolymerization at 80 °C under microwave irradiation. The final monomer conversion and the polymerization rate increase gradually with increasing emulsifier concentrations. It is because the size of the monomer droplets decreases with increasing emulsifier concentrations and number of monomer droplets. In miniemulsion polymerization, each monomer droplet is an individually independent nanoreactor. The places of initiation and propagation increase when the number of monomer droplets increases. Accordingly, the polymerization rate increases. Meanwhile, the emulsifier concentration usually stays well below the critical micelle concentration. If the amount of emulsifier is too little, the emulsifier adsorbed on the surface of latex particles is small and the stability of minimeulsion is not good. If the amount of emulsifier is too much, the residual concentration of the emulsifier in the water phase increases and it presumably leads to

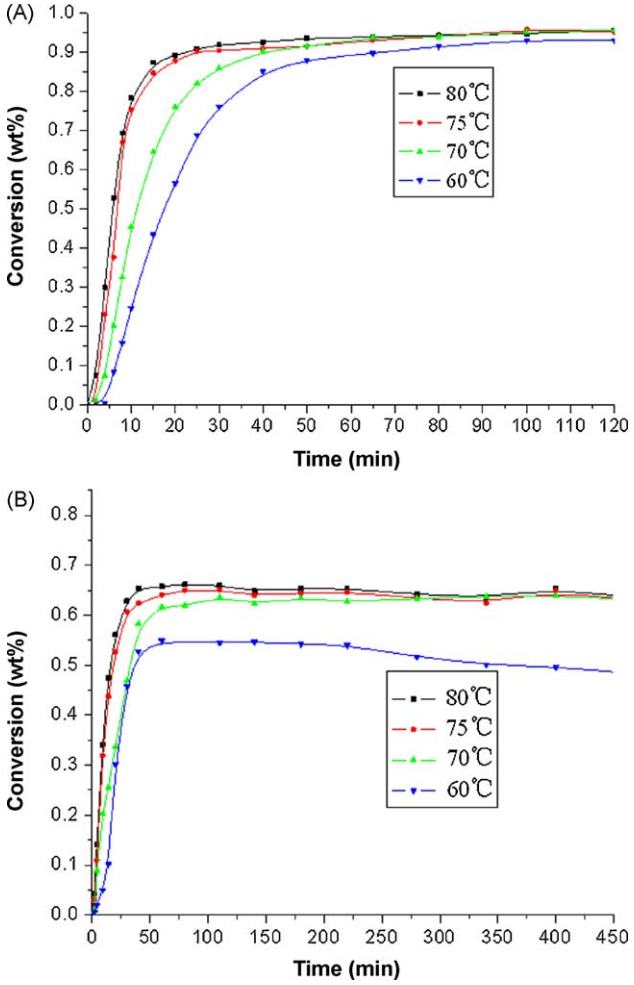

Fig. 6. Effects of the reaction temperature on monomer conversion: (A) under microwave irradiation and (B) under traditional heating (DFHMA, 2.50 g; MMA, 4.00 g; BA, 3.50 g; [AIBN] = 0.5%; emulsifier concentration = 2.5%).

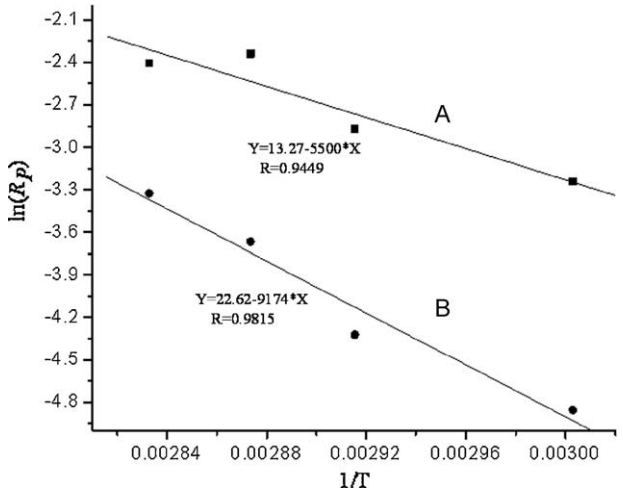

Fig. 7. $\ln(R_p)$ versus $1/T$ (A) under microwave irradiation and (B) under traditional heating.

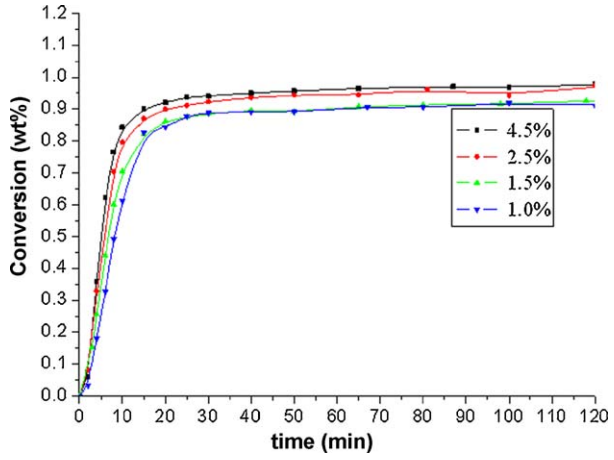

Fig. 8. Effect of emulsifier concentration on monomer conversation (microwave irradiation at 80 °C, 400 W; DFHMA, 2.50 g; MMA, 4.00 g; BA, 3.50 g; [AIBN] = 0.5%).

another mechanism of micelle nucleation. The kinetic plots are shown in Fig. 9 and the relationship obtained from Figs. 8 and 9 shows that R_p is proportional to $[SDS/OP\text{-}10]^{0.328}$, indicating that the rate of miniemulsion polymerization under microwave irradiation within our experiments is proportional to the 0.328 power of the concentration of the emulsifier. Besides, the linear relationships indicating that the growing radical concentration is constant with the change of emulsifier concentrations during the reaction and no significant termination reactions occurred during the polymerization [35], this result is in good agreement with other microwave irradiation miniemulsion polymerization [34].

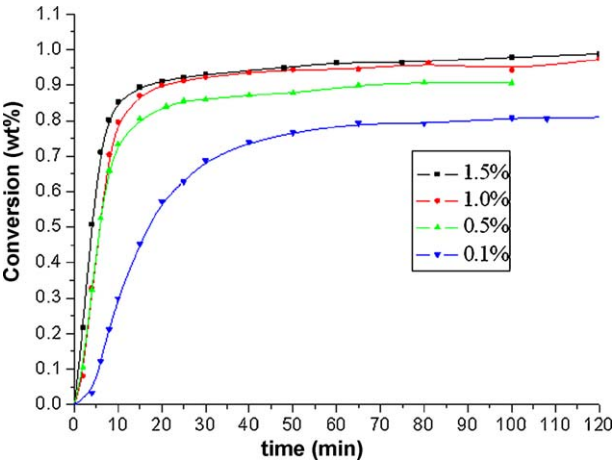

Fig. 10. Effects of AIBN concentration on monomer conversion (microwave irradiation at 80 °C, 400 W; DFHMA, 2.50 g; MMA, 4.00 g; BA, 3.50 g; emulsifier concentration = 2.5%).

Fig. 10 illustrates the effects of the concentration of AIBN (weight percentage of the AIBN with respect to the monomer mixture) on the monomer conversion in miniemulsion polymerization at 80 °C under microwave irradiation. It can be observed that the monomer conversion and polymerization rate increase with AIBN concentrations. It can be attributed to more free radicals initiating the polymerization in every reaction place if the concentration of AIBN increases. Fig. 9 also shows that when the concentration of AIBN is too low (0.1 wt%), both the final conversion of the monomer and the polymerization rate are not very high. The kinetic plots are shown in Fig. 11 and the relationship obtained from Figs. 10 and 11 suggests that R_p is proportional to $[AIBN]^{0.297}$ indicating that the rate of miniemulsion polymerization under microwave irradiation is proportional to the 0.297 power of the concentration of the AIBN within our experiments. The exponent deviates from the theoretical typical value of 0.5 for classical emulsion polymerization, which may

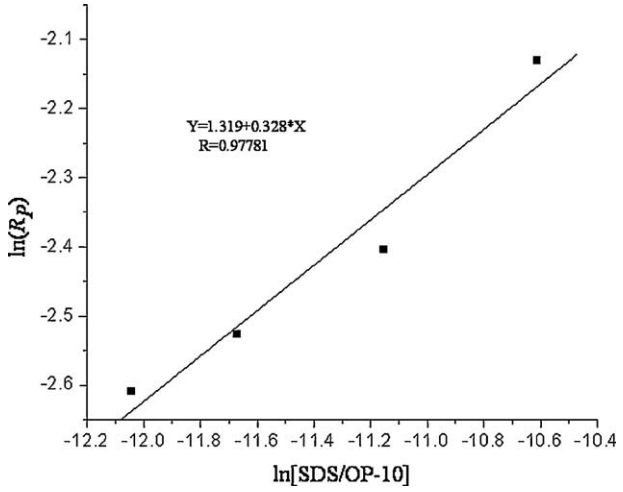

Fig. 9. $\ln(R_p)$ versus ln[SDS/OP-10].

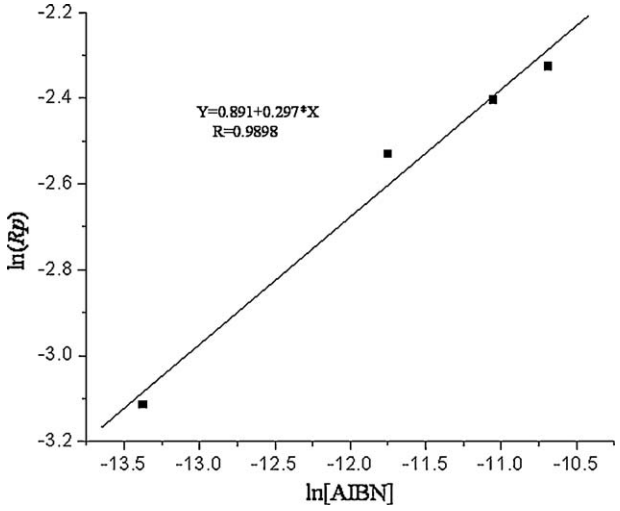

Fig. 11. $\ln(R_p)$ versus ln[AIBN].

Table 3
Effects of the mixed emulsifier system on the centrifugal stability of the miniemulsion.

	Amount of mixed emulsifier (wt%)			
	1	1.5	2.5	4.4
Sedimentation ratio (wt%)[a]	14.79	8.91	2.71	2.48
Sedimentation ratio (wt%)[b]	15.23	9.53	2.82	2.61

[a] The miniemulsion polymerization under microwave irradiation.
[b] The miniemulsion polymerization with traditional heating.

imply that the ratio of active species number to total species particle number in the microwave irradiation miniemulsion polymerization system is higher than classical emulsion polymerization [36,37]. In microwave irradiation polymerization, microwave irradiation enhance the activity of the initiator AIBN by raising its decomposition, and the formation rate of the primary active species in the monomer droplets increases with accelerated decomposition rates of AIBN. Hence, large amounts of active species are formed under microwave irradiation.

2.4. Stability of miniemulsion

The miniemulsion prepared in this work has good storage, dilution, heat-resistance, and cold-resistance stability. The effects of the amount of DFHMA and mixed emulsifier on the centrifugal stabilities are shown in Tables 2 and 3. The higher the sedimentation ratio, the lower is the centrifugal stability of the miniemulsion. Table 2 illustrates that with higher DFHMA amounts, the centrifugal stability of the miniemulsion decreases. Since the intermolecular force of C–F groups is very low, adsorption of the mixed emulsifier on the latex particle surface becomes difficult. Therefore, the small latex particles exhibit a trend to integrate and the large particles are easy to deposit [10]. Table 3 indicates that the centrifugal stability of the miniemulsion increases with higher mixed emulsifier amounts. Small amounts of emulsifier cannot ensure full conversion of the surface of the latex particles, which will decrease the centrifugal stability of the miniemulsion. Table 3 also confirms that the centrifugal stability of the miniemulsion which prepared under microwave irradiation is better than that obtained by traditional heating. It is possible due to the much smaller size of the latex particles obtained by microwave irradiation because smaller particles have large surface areas and adsorb more emulsifier. Therefore, the centrifugal stability of the miniemulsions is better than that achieved by conventional heating miniemulsion.

2.5. Surface property of the latex films

To investigate the surface morphology of the latex films on the nanometer scale, atomic force microscopy (AFM) was used to evaluate the topography of the resulted films. According to the AFM analysis in Fig. 12, the surface appeared "bumpy" with a grainy structure. This is the result of phase separation of the fluoroalkyl segments [9]. It was also observed that the polymer surface was nearly completely covered with fluoroalkyl groups which appeared brighter, and the darker small areas between the grainy structures were referred to the softer non-fluorinated acrylate [38]. Basically, the interaction between acrylate polymers and the polar mica substrate is smaller than the interaction between F-containing groups and mica surface, and acrylate polymers will collapse on a mica surface. In the anneal process the fluoroalkyl groups preferred to migrate to the air/polymer interface and occupy the outmost surface.

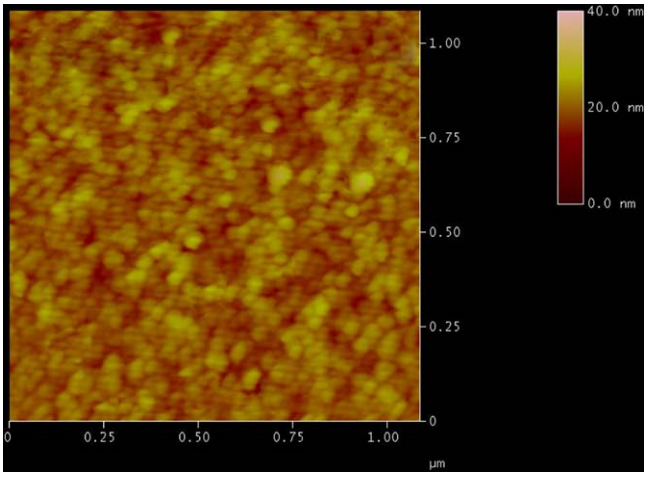

Fig. 12. AFM images of latex particles (A height image with scan size of 1.00 μm × 1.00 μm and scan rate of 2.001 Hz. The latex particles were prepared by miniemulsion polymerization under microwave irradiation at 80 °C, 400 W for 2 h. DFHMA, 2.50 g; MMA, 4.00 g; BA, 3.50 g; HD, 0.40 g; OP-10, 0.17 g; SDS, 0.08 g; AIBN, 0.05 g; H_2O, 40.00 g).

Table 4
Contact angles and surface-free energies of latex films (the latex films were prepared by miniemulsion polymerization under microwave irradiation).

Sample	Amount of DFHMA (wt%)	Contact angles (°)		Surface energy (γ_s) (mJ/m^2)
		Water	Hexadecane	
1	0[a]	89.3	33.5	27.24
2	5[a]	95.0	43.3	23.44
3	10[a]	98.9	64.3	17.59
4	15[a]	100.1	70.3	15.97
5	25[a]	101.4	73.9	14.85
6	15[b]	94.7	39.5	24.34
7	25[b]	95.3	40.3	23.99

[a] indicates the latex films after anneal.
[b] indicates the latex films before anneal.

The contact angles of water and oil on the latex films with different amount of DFHMA are listed in Table 4. The water contact angle of a typical hydrophobic surface is usually above 90°. Although the emulsifier amount, initiator amount, and so on affect the contact angles of water and oil, the amount of DFHMA plays an important role in the surface properties of the latex films.

Table 4 shows that the contact angles of water and hexadecane increase with increasing DFHMA amounts and the surface-free energy decreases. The fluorinated copolymers have lower surface-free energy and incorporation of fluorinated moieties into a polymer film has been shown to be effective in increasing the hydrophobicity of the latex surface. All the fluoroacrylate copolymers exhibit good water/oil-resistant properties. According to the measured contact angles of water and hexadecane, the surface-free energy can be calculated. The surface-free energy of the latex films containing DFHMA is much lower than that of the film without DFHMA. When fluoroalkyl groups with low surface tension are introduced into the copolymer chains, the surface energy of the latex film is greatly reduced and the latex film cannot be wetted by water and oil easily. Table 4 also shows that the surface-free energy of the latex films containing DFHMA diminishes after annealing. It may be attributed to the special properties of the F atoms because accumulation of F-containing groups is increased on the surface of latexes film when annealed which can be seen from the AFM image. In addition, the surface-free energy lessens. In the latex films obtained by miniemulsion polymerization, F-groups accumulate effectively on the surface during film formation. Although the F% on the latex surface reaches

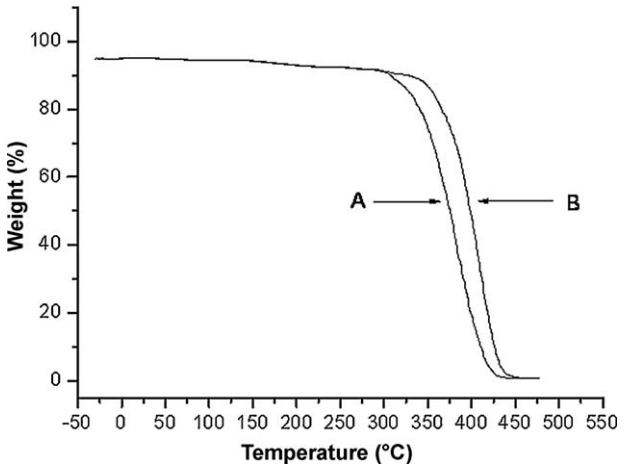

Fig. 13. TGA curves of the latex films: (A) a non-fluorine film (microwave irradiation at 80 °C, 400 W; DFHMA, 0 g; MMA, 5.00 g; BA, 4.00 g) and (B) a fluorine-containing film (microwave irradiation at 80 °C, 400 W; DFHMA, 1.00 g; MMA, 5.00 g; BA, 4.00 g).

the tiptop, the DFHMA amount is still low. Therefore, the contact angles of water and hexadecane do not continue to increase even the amount of DFHMA is further increased.

2.6. Thermal stability of the latex films

The thermo-gravimetric curves of the latex films without and with fluorine are displayed in Fig. 13(A) and (B), respectively. The latex film with 10% DFHMA (weight percentage of the DFHMA with respect to the monomer mixture) begins to decompose at 350 °C and the process is completed at 440 °C. In comparison, the decomposition of the latex film without fluorine begins at 325 °C and ends at 420 °C. After introducing a few fluoromonomers, the decomposition temperature increases by 25 °C indicating that the thermal stability of the latex film is significantly modified. This phenomenon can be attributed to the long-chain perfluoroalkyl groups of DFHMA. The perfluoroalkyl chain containing C–F units has high bond energy and sufficiently shields and protects the non-fluorinated segment beneath the fluorinated segment.

3. Conclusion

Fluoroacrylate copolymer has been successfully prepared by miniemulsion polymerization under microwave irradiation. The results obtained by DSC, FTIR, ^{1}H NMR and ^{19}F NMR indicate that DFHMA takes part in copolymerization. The polymer particles are found to be a one-to-one copy of the monomer droplets and droplet nucleation is the dominant mechanism in polymerization. Copolymerization under microwave irradiation has a higher reaction rate and higher conversion than traditional heating. The centrifugal stability miniemulsion which prepared by microwave irradiation is also much better than those prepared by traditional heating, indicating that polymerization is more successful under microwave irradiation. The TEM images show that latex particles prepared by microwave irradiation miniemulsion polymerization have a spherical morphology and are smaller than 60 nm with a narrow distribution. The average hydrodynamic diameter *Dh* and the poly index of the nanoparticles are measured by PCS. Both the *Dh* and poly index of the nanoparticles prepared by microwave irradiation are much smaller than those of particles prepared by conventional heating. The amount of DFHMA has an important effect on the surface properties of the latex films. The more DFHMA the latex films have, the higher the contact angles to water/oil were and the lower surface-free energy. Moreover, AFM analysis and contact angle measurement on the latex films which after annealing indicated that the propensity of fluorine enrichment at film–air interface, and the surface-free energy of latex films decreases further. In comparison with latex films of fluorine-free polyacrylate, the thermal stability of the fluorinated latex films is evidently enhanced.

4. Experimental

4.1. Materials

Dodecafluoroheptyl methacrylate $CH_2{=}CHCOOCH_2CF(CF_3)CFHCF(CF_3)_2$ (2,4-di(trifluoromethyl)-2,3,4,5,5,5-hexafluoropentyl methacrylate, Actyflon-G04 or DFHMA) was purchased from XEOGIA Fluorine-Silicon Chemical Co. (Harbin, China, chemical purity) and was distilled under reduced pressure before use. Methyl methacrylate (MMA) and n-butyl acrylate (n-BA) purchased from Shanghai Chemical Reagents Co. (Shanghai, China, chemical purity) were distilled under vacuum and stored at 5 °C. Sodium dodecylsulfate (SDS) and polyoxyethylene alkylphenol ether (OP-10) (Shanghai Chemical Reagents Co., chemical purity) serving as the mixed emulsifiers were used as received. Hexadecane (HD) was provided by ABCR and used as received. The initiator 2,2′-azobisisobutyronitrile (AIBN) was purified by recrystallization in ethanol. Deionized water was used in all the polymerization and treatment processes.

4.2. Apparatus

The apparatus used for miniemulsion copolymerization was an XH-100A microwave oven purchased from Beijing XianHu Science and Technology Development Co., Ltd. The microwave frequency was 2.45 GHz and the output power was continuously adjustable within the range of 100–1000 W. The temperature can be controlled in real time by a temperature-sensitive sensor. A 100 mL, four-necked, round bottom flask equipped with a reflux condenser, Teflon paddle stirrer, temperature sensor, and nitrogen gas inlet were fixed in the microwave oven. The reaction apparatus is schematically presented in Fig. 14.

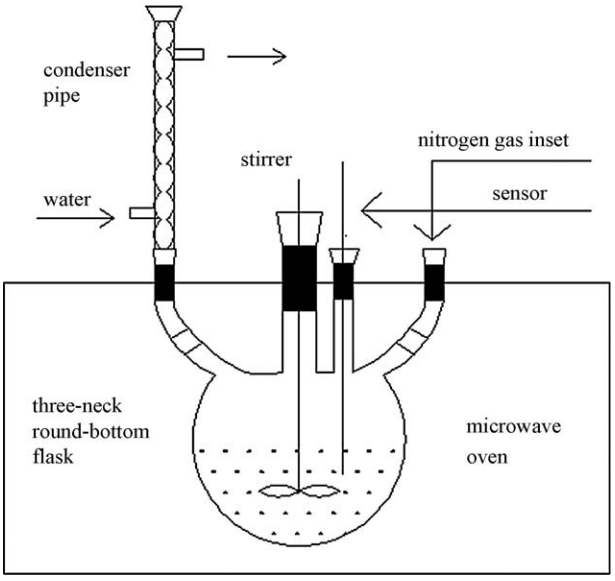

Fig. 14. Schematic of the reaction apparatus for microwave irradiation.

4.3. Miniemulsion copolymerization

4.3.1. Miniemulsion polymerization under microwave irradiation

The monomers miniemulsion was prepared according to the following procedures. The monomer mixture containing MMA, BA, and DFHMA were first mixed with HD. The mixture was then added to the aqueous phase (water, OP-10, SDS [OP-10 Wt:SDS Wt = 1:2)] under stirring. After 20 min, the resultant emulsion was homogenized by ultrasonication for 240 s with 30% amplitude at 0 °C to prevent polymerization. The final miniemulsion was transferred to a 100 mL glass reactor placed on the center of the rotating table in a microwave oven. Before the reaction started, the reactor was purged with nitrogen for 60 min. Then AIBN dissolved in 5 g water was added to the reactor and the system was kept under nitrogen atmosphere until polymerization was completed. The reaction system was irradiated with microwave (400 W) for 2 h at a prescribed temperature. The reaction kinetics was studied by taking samples (quenched with hydroquinone) from the system at regular time intervals and the conversion of polymerization was determined gravimetrically based on the samples taken during the process. A typical miniemulsion polymerization under microwave irradiation comprise 40.00 g of water, 0.40 g of HD, 0.25 g of mixed emulsifier (OP-10 Wt:SDS Wt = 1:2), 2.50 g of DFHMA, 4.00 g of MMA, 3.50 g of BA, and 0.05 g of AIBN. In that case, the theoretic solid content was close to the expected 21.1%.

4.3.2. Miniemulsion polymerization with traditional heating

The general procedure was the same as microwave polymerization. The polymerization was carried out at 80 °C for 8 h to obtain stable latex.

4.4. Measurements

4.4.1. Polymerization characterization

Conversion was measured by gravimetric analysis [16]. At regular time intervals a certain quantity of emulsion was cast into a Petri dish (quenched with hydroquinone) and dried to a constant weight in a dry oven at 75 °C. Conversion was calculated by the following formulas:

$$\text{solid content}(\text{wt}\%) = \frac{W_2 - W_0}{W_1 - W_0} \times 100\% \quad (1)$$

$$\text{conversion}(\text{wt}\%) = \frac{[W_3 \times \text{solid content}\%] - W_4}{W_5} \times 100\% \quad (2)$$

where W_0 is the weight of the Petri dish, W_1 and W_2 are the weight of emulsion before and after drying to a constant weight, W_3 is the total weight of all the materials put in glass reactor in each polymerization, W_4 is the weight of materials that cannot volatilize when drying, and W_5 is the total weight of monomers, respectively.

4.4.2. Structural characterization

Dried samples of the latexes were obtained from precipitation in ethanol. The filtered latexes were washed several times with water and ethanol to remove emulsifiers and then dried in a vacuum oven at an elevated temperature. IR spectra of the copolymers were recorded on a Perkin-Elmer Spectrum One FTIR spectrometer (Perkin-Elmer Co., USA). All the ^{1}H NMR and ^{19}F NMR spectra were recorded using a UNITY INVOA-600 MHz spectrometer (Varian, USA) with $CDCl_3$ as the solvent at room temperature. The copolymer compositions were calculated from the characteristic proton integrals. The glass-transition temperature of the copolymer was measured by differential scanning calorimetry (DSC) in the range from −50 to 200 °C with a Perkin-Elmer DSC 7 differential scanning calorimeter (Perkin-Elmer Co., USA) under nitrogen atmosphere at the heating rate of 20 °C/min.

4.4.3. Particle size characterization

The data for the average monomer droplet and latex particle size during polymerization were obtained by the photon correlation spectroscopy (PCS) (Malvern Zetasizer Nano S, UK).

4.4.4. Transmission electron microscopy (TEM)

The morphology of the latex particles was characterized by transmission electron microscopy (TEM) (Tecnai G20, FEI Corp., USA). The latex particles which prepared by microwave irradiation miniemulsion polymerization (at 80 °C, 400 W for 2 h) and conventional heating miniemulsion polymerization (at 80 °C for 8 h) were diluted to 0.3%, applied to a 400-mesh, carbon-coated copper grid, and left to dry at room temperature. The diameters of more than 100 microspheres were measured from the TEM images. The number average diameter (D_n), weight-average diameter (D_w), and the polydispersity index (PDI) were calculated as follows:

$$D_n = \frac{\sum_{i-1}^{k} N_i D_i}{\sum_{i-1}^{k} N_i} \quad (3)$$

$$D_w = \frac{\sum_{i-1}^{k} N_i D_i^4}{\sum_{i-1}^{k} N_i D_i^3} \quad (4)$$

$$PDI = \frac{D_w}{D_n} \quad (5)$$

where N_i is the number of microspheres with diameter D_i.

4.4.5. Stability of the miniemulsion

The centrifugal stability of the miniemulsion was determined by a centrifugal method (12,000 rpm, 60 min.). The sedimentation ratio was calculated using the following formula: sedimentation ratio (wt%) = $W_1/W_0 \times 100\%$, where W_1 is the weight of the sedimentation and W_0 is the weight of the original samples.

4.4.6. Film formation and characterization

The surface property of the resulted copolymers films was studied using dynamic contact angle and atomic force microscopy (AFM). The latex films were prepared by the casting method by spreading the obtained miniemulsion directly on a new-cleaned glass plate and dried at room temperature. Parts of the dried films were annealed for 4 h at 120 °C and then kept in an oven at room temperature under vacuum before contact angles measurement. The same unannealed latexes films were used for the thermal stability analysis. And in the case of atomic force microscopy (AFM) measurement, the samples were prepared by spin coating from a dilute emulsion of polymer onto a freshly cleaved mica surface. To further promote the migration of perfluorinated side chains, the films were annealed for 4 h at 120 °C and then kept in an oven at room temperature under vacuum.

The dynamic contact angles data were obtained by Wilhelmy method [39] at 25 °C using a Krŭss interface tension meter (Krŭss GmbH, Hamberg, Germany). The sample was held in the microbalance and progressively immersed in water and conversely receded to its original position at a constant rate of 0.5 mm/s. The surface-free energy of the polymers was calculated using the measured contact angles for various liquids by Eqs. (6) and (7):

$$\gamma_{\text{solid}} = \gamma^d_{\text{solid}} + \gamma^p_{\text{solid}} \quad (6)$$

$$\gamma_{\text{liquid}}(\cos\theta + 1) = 2(\gamma^d_{\text{solid}}\gamma^d_{\text{liquid}})^{1/2} + 2(\gamma^p_{\text{solid}}\gamma^p_{\text{liquid}})^{1/2} \quad (7)$$

Here, γ is the surface-free energy and the superscripts d and p correspond to dispersion and polar components of the surface-free energy, respectively. The wetting liquids used for contact angle measurements were water and hexadecane. The γ, γ^d and γ^p for

water were 72.8, 21.8 and 51.0 mJ/m^2 and for hexadecane were 27.6, 27.6 and 0 mJ/m^2, respectively. The contact angles to hexadecane were also measured as the index of oleophobicity of the latex films. AFM measurements were obtained with a Nanoscope IIIa (Digital Instrument, Santa Barbara, CA) at room temperature, the measurements were made in the tapping mode.

4.4.7. Thermal stability of the latex films

Thermal degradation was investigated by thermo-gravimetric analysis performed on a TGA7 from Perkin-Elmer Corporation which recorded the total weight loss on approximately 10–12 mg of samples from room temperature to 600 °C at a rate of 5 °C/min under a continuous nitrogen flow of 90 mL/min.

Acknowledgments

The work was jointly supported by the Key Projects in the National Science & Technology Pillar Program during the Eleventh Five-year Plan Period (No. 2008BAC32B03) and Hong Kong Research Grants Council (RGG) General Research Funds (GRF) (No. CityU 112306).

References

[1] B. Baradie, M.S. Shoichet, Macromolecules 38 (2005) 5560–5568.
[2] J.L. He, P.H. Ni, C.C. Liu, J. Polym. Sci., Part A: Polym. Chem. 46 (2008) 3029–3041.
[3] J.R. Lee, F.L. Jin, S.J. Park, J.M. Park, Surf. Coat. Technol. 180–181 (2004) 650–654.
[4] R. Morent, N. DeGeyter, J. Verschuren, K. DeClerck, P. Kiekens, C. Leys, Surf. Coat. Technol. 202 (2008) 3427–3449.
[5] D.R. Iyengar, S.M. Perutz, C. Dai, C.K. Ober, E.J. Kramer, Macromolecules 29 (1996) 1229–1234.
[6] F. Signori, M. Lazzari, V. Castelvetro, O. Chiantore, Macromolecules 39 (2006) 1749–1758.
[7] P.Y. Huang, Y.C. Chao, Y.T. Liao, J. Appl. Polym. Sci. 94 (2004) 1466–1472.
[8] I.J. Park, S.B. Lee, C.K. Choi, Macromolecules 31 (1998) 7555–7558.
[9] T.T. Yang, L. Yao, H. Peng, S.Y. Cheng, I.J. Park, J. Fluorine Chem. 127 (2006) 1105–1110.
[10] Y.J. Chen, S.Y. Cheng, Y.F. Wang, C.C. Zhang, J. Appl. Polym. Sci. 99 (2006) 107–114.
[11] J.Q. Huang, W.D. Meng, F.L. Qing, J. Fluorine Chem. 128 (2007) 1469–1477.
[12] J. Guo, P. Resnick, K. Efimenko, J. Genzer, J.M. DeSimone, Ind. Eng. Chem. Res. 47 (2008) 502–508.
[13] N.M.L. Hansen, K. Jankova, S. Hvilsted, Eur. Polym. J. 43 (2007) 255–293.
[14] J.W. Ha, I.J. Park, S.B. Lee, D.K. Kim, Macromolecules 35 (2002) 6811–6818.
[15] Q.H. Zhang, X.L. Zhan, F.Q. Chen, J. Appl. Polym. Sci. 104 (2007) 641–647.
[16] Y.J. Chen, C.C. Zhang, X.X. Chen, Eur. Polym. J. 42 (2006) 694–701.
[17] K.L. Xie, A.Q. Hou, Y.Q. Shi, J. Appl. Polym. Sci. 108 (2008) 1778–1782.
[18] L.B. Du, J.Y. Kelly, G.W. Roberts, J.M. DeSimone, J. Supercrit. Fluids 47 (2009) 447–457.
[19] X.Y. Xiao, Y. Wang, Colloids Surf. A: Physicochem. Eng. Aspects 348 (2009) 151–156.
[20] K. Landfester, Macromol. Rapid Commun. 22 (2001) 896–936.
[21] N. Bechthold, K. Landfester, Macromolecules 33 (2000) 4682–4689.
[22] J.M. Asua, Prog. Polym. Sci. 27 (2002) 1283–1346.
[23] J.W. Ha, I.J. Park, S.B. Lee, Macromolecules 38 (2005) 736–744.
[24] T.Y. Guo, D.L. Tang, M.D. Song, B.H. zhang, J. Polym. Sci., Part A: Polym. Chem. 45 (2007) 5067–5075.
[25] J. Adams, A. Hardin, F. Vounatsos, J. Org. Chem. 71 (2006) 9895–9898.
[26] D. Samaroo, C.E. Soll, L.J. Todaro, C.M. Drain, Org. Lett. 8 (2006) 4985–4988.
[27] W.S. Bremner, M.G. Organ, J. Comb. Chem. 9 (2007) 14–16.
[28] J. Canadell, A. Mantecón, V. Cádiz, J. Polym. Sci., Part A: Polym. Chem. 44 (2006) 4722–4730.
[29] W.M. Zhang, J. Gao, C. Wu, Macromolecules 30 (1997) 6388–6390.
[30] J.L. Huang, Y.L. Zhang, Z.H. Cheng, H.C. Tao, J. Appl. Polym. Sci. 103 (2007) 358–364.
[31] R. Hoogenboom, U.S. Schubert, Macromol. Rapid. Commun. 28 (2007) 368–386.
[32] C. Holtze, M. Antonietti, K. Tauer, Macromolecules 39 (2006) 5720–5728.
[33] C. Holtze, K. Tauer, Macromol. Rapid. Commun. 28 (2007) 428–436.
[34] J.A. Li, X.L. Zhu, J. Zhu, Z.P. Cheng, Radiat. Phys. Chem. 76 (2007) 23–26.
[35] M. Fernández-Garcia, P.F. Canamero, J.L. Fuente, React. Funct. Polym. 68 (2008) 1384–1391.
[36] Z. Qian, J. Chen, Y. Chen, Z.C. Zhang, H.R. Liu, Colloids Surf. A: Physicochem. Eng. Aspects 295 (2007) 7–15.
[37] D.A. Lewis, J.D. Summers, T.C. Ward, J.E. McGrath, J. Polym. Sci., Part A: Polym. Chem. 30 (1992) 1647–1653.
[38] L. Zhang, C.F. Oh, Surf. Interface Anal. 38 (2006) 949–956.
[39] A.H. Hogt, D.F. Gregonia, J.D. Andrade, J. Colloid lnterface Sci. 106 (1985) 289–298.